ELSEVIER

Contents lists available at ScienceDirect

### European Journal of Pharmaceutical Sciences

journal homepage: www.elsevier.com/locate/ejps



## The potential of enteroids derived from children and adults to study age-dependent differences in intestinal CYP3A4/5 metabolism

Eva J. Streekstra <sup>a,b</sup>, Marit Keuper-Navis <sup>b,c</sup>, Jeroen J.W.M. van den Heuvel <sup>a</sup>, Petra van den Broek <sup>a</sup>, Rick Greupink <sup>a</sup>, Martijn W.J. Stommel <sup>d</sup>, Willem P. de Boode <sup>e</sup>, Sanne M.B.I. Botden <sup>f</sup>, Frans G.M. Russel <sup>a</sup>, Evita van de Steeg <sup>b,1</sup>, Saskia N. de Wildt <sup>a,g,h,1,\*</sup>

- <sup>a</sup> Division of Pharmacology and Toxicology, Department of Pharmacy, Radboud University Medical Center, Nijmegen, the Netherlands
- b Department of Metabolic Health Research, Netherlands Organization for Applied Scientific Research (TNO), Leiden, the Netherlands
- <sup>c</sup> Division of Pharmacology, Utrecht Institute for Pharmaceutical Sciences (UIPS), Utrecht University, Utrecht, the Netherlands
- <sup>d</sup> Department of Surgery, Radboud University Medical Center, Nijmegen, the Netherlands
- e Department of Pediatrics, Division of Neonatology, Radboud University Medical Center, Amalia Children's Hospital, Nijmegen, the Netherlands
- <sup>f</sup> Amalia Children's Hospital, Radboud University Medical Center, Nijmegen, the Netherlands
- <sup>g</sup> Department of Intensive Care, Radboud University Medical Center, Nijmegen, the Netherlands
- h Department of Neonatal and Pediatric Intensive Care, Erasmus MC Sophia Children's Hospital, Rotterdam, the Netherlands

#### ARTICLE INFO

# Keywords: Intestine Intestinal organoids Enteroids Pediatrics Ussing chamber Pharmacokinetics Drug metabolizing enzymes

#### ABSTRACT

Drug metabolism in the intestinal wall affects bioavailability of orally administered drugs and is influenced by age. Hence, it is important to fully understand the drug metabolizing capacity of the gut to predict systemic exposure. The aim of this study was to investigate the potential of enteroids as a tool to study CYP3A4/5 -mediated metabolism in both children and adults.

Bioconversion of midazolam, a CYP3A4/5 model substrate, was studied using enteroid monolayers as well as tissue explants in the Ussing chamber, both derived from pediatric [median (range age): 54 weeks (2 days - 13 years), n=21] and adult (n=5) tissue. Caco-2 cellular monolayers were employed as controls. In addition, mRNA expression of CYP3A4 was determined in enteroid monolayers (n=11), tissue (n=23) and Caco-2 using RT-qPCR.

Midazolam metabolism was successfully detected in all enteroid monolayers, as well as in all tissue explants studied in the Ussing chamber, whereas Caco-2 showed no significant metabolite formation. The extracted fraction of midazolam was similar between enteroid monolayers and tissue. The fraction of midazolam extracted increased with age in enteroid monolayers derived from 0 to 70 week old donors. No statistically significant correlation was observed in tissue likely due to high variability observed and the smaller donor numbers included in the study. At the level of gene expression, CYP3A4 increased with age in tissues (n=32), while this was not reflected in enteroid monolayers (n=16). Notably, asymmetric metabolite formation was observed in enteroids and tissue, with higher metabolite formation on the luminal side of the barrier.

In summary, we demonstrated that enteroids can be used to measure CYP3A4/5 midazolam metabolism, which we show is similar as observed in fresh isolated tissue. This was the case both in children and adults, indicating the potential of enteroids to predict intestinal metabolism. This study provides promising data to further develop enteroids to study drug metabolism *in vitro* and potentially predict oral absorption for special populations as an alternative to using fresh tissue.

#### 1. Introduction

Most drugs are prescribed for oral administration to patients, making

the intestine the first site of drug exposure and a key determinant of drug pharmacokinetics (PK). Drug metabolism in the intestinal wall (part of the first-pass effect) can result in altered bioavailability of oral

https://doi.org/10.1016/j.ejps.2024.106868

<sup>\*</sup> Corresponding author at: P.O. Box 9101, 6500 HB Nijmegen, the Netherlands. E-mail address: Saskia.dewildt@radboudumc.nl (S.N. de Wildt).

<sup>&</sup>lt;sup>1</sup> E. van de Steeg and S.N. de Wildt share last authorship.

administered drugs (Doherty and Charman, 2002). Age is a factor described to play a role in the drug metabolizing capacity (Nicolas et al., 2017). Hence, it is important to fully understand the drug metabolizing functionality of the gut to better predict systemic exposure in patients of different age groups.

To study intestinal metabolism, researchers currently depend on residual tissue from surgeries or conventional *in vitro* cell models. Fresh tissue is hard to work with, as available samples are often very small and susceptible to variation due to handling and external exposures. Conventional *in vitro* models, like Caco-2 cells have limited potential to predict oral drug bioavailability; they lack accurate enzyme expression and functionality. Innovative approaches, such as tissue-derived intestinal organoids (enteroids) may present a better way to investigate drug metabolism *in vitro* compared to the use of primary tissues, while at the same time being a more relevant system as compared to cultured cell lines (Sato and Clevers, 2013).

Human enteroids can be derived from small pieces of tissue and keep epigenetic properties of the patient, including disease and probably age, as has been shown in DNA methylation studies (Kraiczy et al., 2019; Lewis et al., 2020). Once isolated, they can be expanded and maintained in culture for several months. Initially, enteroids grow in a self-organizing 3D formation with a hollow inside representing the luminal side of the intestine. This makes it hard to mimic oral exposure in enteroids. Yet, enteroids can also be cultured in a monolayer formation on a permeable membrane insert, allowing exposure to drugs from the luminal side. This enables the comparison of the contribution of drug metabolism to intestinal absorption between enteroid monolayers and tissue (using Ussing chamber) (Altay et al., 2019; Braverman and Yilmaz, 2018; Gunasekara et al., 2018; Roodsant et al., 2020; Scott et al., 2016; Speer et al., 2019a, 2019b; Takenaka et al., 2016; Wang et al., 2017; Yamashita et al., 2021).

Growth and development during a child's lifespan affect the pharmacokinetics of a drug, limiting extrapolation of dosing from adults (van den Anker et al., 2018). Although the intestine is the first site of drug exposure after oral dosing, studies with a focus on intestinal drug metabolizing enzyme (DME) functionality in the pediatric age group are scarce. Variation in DME functionality, caused by maturational changes, is an important factor influencing bioavailability of an orally dosed drugs, especially during the first year of life (Nicolas et al., 2017; van Groen et al., 2021b). For example, midazolam clearance appears to be lower and oral bioavailability higher in preterm infants compared to children above one year of age (Brussee et al., 2018a, 2018b; de Wildt et al., 2002). However, the exact contribution of Cytochrome P450 enzyme (CYP) 3A-mediated intestinal metabolism relative to the other main site of (first-pass) metabolism, the liver, is unknown. CYP3A4 is one of the most abundantly expressed drug metabolizing enzymes (DME) in the intestine, responsible for metabolizing many drugs (Paine et al., 1996). While CYP3A4 protein abundance increases in the small intestine with increasing age, data on intestinal CYP3A4/5 functionality with age are scarce (de Waal et al., 2024; Goelen et al., 2023; Kiss et al., 2021; Streekstra et al., 2022). Studying metabolism in fresh tissue (Ussing chamber) from children is the golden standard, but this methodology is vulnerable due to the limited tissue availability, size and viability (Streekstra et al., 2022). With the use of enteroids derived from children we may be able to bridge this gap.

In this study we aimed to demonstrate the potential of enteroids as a tool to study drug metabolism by CYP3A4/5, compared to metabolism in tissue (Ussing chamber) and Caco-2. Additionally, the impact of age on midazolam metabolism was investigated.

#### 2. Methodology

#### 2.1. Human tissues

Surgical leftovers of mid-terminal ileum tissues were collected from pediatric donors undergoing intestinal surgeries at Radboud University

Medical Center (Radboudumc) in Nijmegen, the Netherlands, from 2020 to 2023. The majority of the intestinal material originated from stoma closure at the level of the ileum, details on exact reason for surgery and underlying disease for each can be found in Table A.1. For the inclusion of pediatric donors in the study, informed consent was obtained from parents/legal guardians and/or the children for the use of leftover material and access to clinical data. The need for formal ethics approval was waived in accordance with the Dutch Law on Human Research.

Ileum tissue from adult donors was obtained from (hemi)colectomy surgeries (n=7) between 2020 and 2023. For this, no informed consent was necessary for the use of anonymous leftover material for research purposes, in adherence to the Dutch Code of Conduct for Responsible Use.

After surgical resection, intestinal tissue was transported to the lab within 15 min, in ice cold Krebs buffer. In the lab, the intestinal mucosa was separated from muscle and serosal layers as much as possible. Part of tissue was used for the Ussing chamber experiment, another part was put in storage buffer for enteroid culture. The remainder was snap frozen for later RNA isolation.

#### 2.2. Enteroid culture

#### 2.2.1. 3D culture

The procedures were conducted in accordance with the Stemcell IntestiCult™ protocol and previously established methodologies (14, 18–20). In short, crypts were isolated from tissue specimens within 24-hours post-collection. The protocols for isolation and maintenance of enteroid cultures were derived from previously documented methodologies (Driehuis et al., 2020; Sato et al., 2011). In summary, the mucosal tissue was separated from the muscular and serosal layers, cut into 2–3 mm fragments, and thoroughly rinsed with wash buffer (specific compositions on buffers are available in the Table A.2). Subsequently, crypts were harvested after 1 hour in a crypt-releasing solution. Crypts were seeded in Matrigel (Corning) droplets of 30 µl and provided with 300 µl of Organoid Growth Medium (OGM). The medium was refreshed every 2–3 days, and after a period of 5–10 days, the cultures underwent either mechanical or enzymatic passage, as defined below for monolayer seeding.

#### 2.2.2. 2D monolayers

After 5–10 days, enteroids (P1-P15) were harvested in Advanced DMEM+++ (Table A.2), centrifuged, and dissociated into single cells using TripLE for up to 10 min at 37  $^{\circ}\text{C}$  along with mechanical disruption. The cells were then seeded on 0.1 % acetic acid Collagen 1 (rat tail) coated transparent membrane inserts (6.5 mm, 0.4  $\mu m$  pore size) at a concentration of 1  $\times$  10  $^{5}$  cells per well in OGM. Basolateral medium was added immediately after seeding. Every 2–3 days, the OGM was refreshed. Once confluency of the monolayer was confirmed through microscopic examination and/or measurement of Trans Epithelial Electrical Resistance (TEER), the culture medium was switched to IntestiCult human Organoid Differentiation Medium (ODM), with refreshments every 2–3 days. After 5 days of differentiation the midazolam metabolism assay was performed, as described below.

#### 2.3. Caco-2 monolayer

Human colorectal adenocarcinoma cells (Caco-2) (ATCC, Manassas, VA, US) were grown in supplemented DMEM (10 % fetal calf serum, 1 % non-essential amino acids, 1 % pen/strep). Monolayers were seeded on permeable membrane inserts after cells reached at 80 % confluency (1  $\times$  10  $^5$  cells/well, 6.5 mm, 0.4  $\mu m$  pore size). Medium was refreshed every 2–3 days. After 21 days of culture, the midazolam metabolism assay was performed, as described below.

#### 2.4. Bidirectional metabolism assay in enteroid and Caco-2 monolayers

TEER was measured before and after the experiment to monitor

integrity. Midazolam in transport buffer (10 µM) was added to the donor side of the well after which  $50\,\mu\text{L}$  samples were taken at the acceptor side at t = 0, 30, 60 and 120 min and at the donor side at t = 0 and t = 120min. Fluorescein-dextran 4 kDa (FD4, 50  $\mu$ M) was added to the apical compartment of each insert in order to assess cellular monolayer integrity throughout the length of the experiment. In order to investigate inhibition of CYP3A-mediated metabolism, small intestinal enteroid monolayers were pre-incubated for 30 min with ketoconazole (5 µM) at both apical and basolateral side. During the experiment, cellular monolayers were placed on a rocker at a speed of 70 rpm and maintained at 37 °C. Subsequent to the experiment, integrity was visually assessed and FD4 transport was evaluated. Cellular lysates were collected for intracellular drug quantification, RNA analysis, and protein determinations. Midazolam, 10H-midazolam and 10H-midazolam-glucoronide was measured using Liquid chromatography tandem mass spectrometry (LC-MS/MS). Since midazolam may also appear on the serosal site of the intestine, we also conducted a set of experiments in which enteroid monolayers and tissue were exposed basolaterally, after which appearance of the metabolite 10H-midazolam was measured in both the apical and basolateral compartments.

#### 2.5. Ussing chamber

The exact methods of the Ussing chamber experiments using human intestinal tissues were previously described by Streekstra and Kiss et al., 2022 (Streekstra et al., 2022). In brief, the mucosal barrier was vertically positioned between two chambers, providing an effective surface area of either 0.2 cm² (pediatrics) or 0.71 cm² (adults). Both chambers were filled with Krebs buffer containing N-acetylcysteine (700  $\mu g/mL)$  with continuous carbonation at 37 °C. The viability of the tissue was assessed via electrophysiological monitoring throughout the entirety of the experiment. Following a stabilization period of 15–30 min, the buffer was exchanged for pre-warmed transport buffer containing 10  $\mu M$  of midazolam with dose solution on the apical or basolateral side.

Samples (50  $\mu L)$  were collected at 15-minute intervals for up to two hours. After the experiment tissue slides from the Ussing chamber were washed and snap frozen for further analysis of midazolam and metabolites within the tissue, as well.

#### 2.6. LC-MS/MS

Midazolam and its metabolites 10H-midazolam and 10H-midazolamglucuronide concentrations were determined in the apical, basolateral and tissue/cell lysate compartments of the models used. Sample preparation was applied by protein precipitation in sirocco 96-well filtration plates (Waters, Milford, MA, USA). Every measurement included a standard curve which underwent the exact same sample preparation as the experimental samples. The filtrate was collected in a 96-well plate and 1 µl of the samples was directly injected into the LC-MS/MS system for analysis. Midazolam, 10H-midazolam and 10H-midazolam-glucuronide were quantified with LC-MS/MS, using an Acquity UPLC (Waters, Milford, MA, USA) coupled to a Xevo TQ-S (Waters) triple quadrupole mass spectrometer. The compounds were separated on a HSS T3 analytical column (1.8  $\mu m;\,100\times2.1$  mm, Acquity UPLC®, Waters, Ireland). The elution gradient was as follows: 0 – 1,5 min, from 0 % B to 100 % B; 1,5 – 4 min, 100 % B; and 4 -5 min, 0 % B. Solvent A and B consisted of 0.1 % formic acid in H2O and 0.1 % formic acid in Acetonitril, respectively. The column temperature was set at 40  $^{\circ}$ C, and the flow rate was 300  $\mu$ l/min. The effluent from the UPLC was passed directly into the electrospray ion

source. Positive electrospray ionization was achieved using nitrogen as a desolvation gas with ionization voltage at 600 Volt. The source temperature was set at 500 °C and argon was used as collision gas. Detection of all the compounds were based on isolation of the protonated molecular ion, [M+H]+ and subsequent MS/MS fragmentations were carried out. Multi reaction monitoring (MRM) with the following transitions were used: for midazolam m/z 325.9 (parent ion) to m/z 291.0 and 208.9 (both product ions), for 1-hydroxy midazolam m/z 341.9 (parent ion) to m/z 324.0 and 203.0 (both product ions), and for 1-hydroxy midazolam-glucuronide m/z 518.0 (parent ion) to m/z 324.0 and 203.0 (both product ions), for d5-enalaprilate m/z 354.2 (parent ion) to m/z 211.1 and 95.9 (both product ions) and for labetalol m/z 329.2 (parent ion) to m/z 91.0 (product ion).

#### 2.7. RT-qPCR

RNA was isolated from enteroid monolayers and Caco-2 monolayers (collected after the metabolism experiments) as well as fresh snap frozen tissue using the Qiagen RNeasy mini kit according to protocol. Gel electrophoresis was used to check the integrity of all RNA isolates. Afterwards, we processed cDNA with RT-PCR super mix (Bio-Rad). qPCR was performed using TaqMan<sup>TM</sup> Universal PCR Master Mix, primers, probes and its protocol on a CFX Connect<sup>TM</sup> Real-Time System (Bio-Rad). For CYP3A4 the TaqMan<sup>TM</sup> primer probe Hs00604506\_m1 was used. We used Villin-1 (Hs01031739\_m1) to normalize for enterocyte input of tissue and enteroids (Goelen et al., 2023; Johnson et al., 2001; Kiss et al., 2021; Mooij et al., 2016, 2014), as tissue biopsies used for RNA isolation may consist of a lamina propria in contrast to enteroid monolayers, which only consist of the epithelial cell layer. The data were analyzed using the delta Ct method and expressed as relative expression with  $2^{-\Delta Ct}$  or fold change with  $\Delta\Delta Ct$  method.

#### 2.8. Immunofluorescence

A list of all antibodies and buffers used can be found in Table A.3. Paraformaldehyde-fixed tissue was embedded in paraffin and sectioned. PFA-fixed enteroid monolayer cultures were first embedded in Histo-Gel<sup>TM</sup> and subsequently embedded in paraffin before sectioning. Slides were deparaffinized and rehydrated, followed by antigen retrieval for 20 min at 95 °C in Tris-EDTA buffer. After blocking with goat serum for 1 hour at room temperature, binding of primary antibodies in wash buffer (1:100) was allowed overnight at 4 °C. Slides were washed and staining was visualized with Alexa-conjugated secondary antibodies (1:100, 1 hour at RT) combined with DAPI, after which slides were mounted with ProLong Gold antifade reagent. Primary and secondary only controls were included to confirm specificity. Images were acquired using Axio observer microscope (ZEISS) and processed with ZEN 2.3 pro (ZEISS).

#### 2.9. Calculations

Midazolam and metabolite concentrations were converted to absolute amounts in pmol per compartment for further calculations. Next, the amount of midazolam metabolized by CYP3A4/5 was calculated as extracted fraction (equation 1). As this fraction is independent from tissue area or mg protein present in the model used, this allows direct comparison of metabolic capacity measured in the enteroid monolayers and Ussing chamber (Nishimura et al., 2007; Paine et al., 1996).

Amount of 10Hmidazolam

Intestinal extracted fraction =  $\frac{1}{\text{Amount of 1OHmidazolam + amount of midazolam available for intestinal metabolism}}$ 

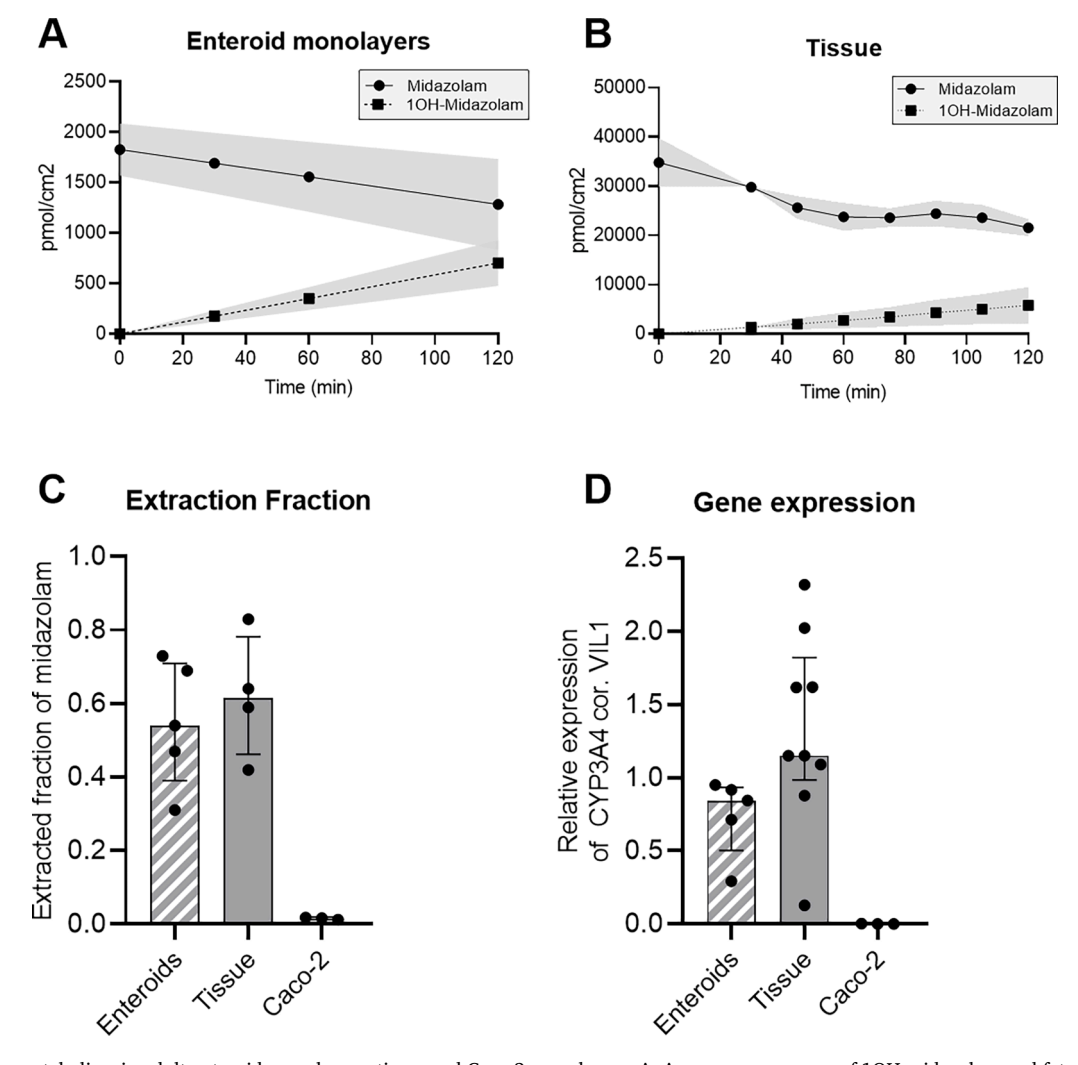


**Fig. 1.** Midazolam metabolism in adult enteroid monolayers, tissue and Caco-2 monolayers. A: Average appearance of 10H-midazolam and fate of midazolam over time in enteroid monolayers (n = 5). B: Average fate of midazolam and appearance of 10H-midazolam over time in adult ileum tissues after apical midazolam dosing (n = 4). C: Metabolic rate in enteroids (n = 5), tissue (n = 4) and Caco-2 cells (n = 3) in median  $\pm$  IQR. D: Gene expression of CYP3A4 in enteroid monolayers (n = 5), tissue (n = 9) and Caco-2 cells (n = 3) corrected for the enterocyte marker Villin-1, in median  $\pm$  IQR.

Where the amount of 1OH-midazolam formed equals the total amount of 1OH-midazolam in pmol in donor, acceptor and cell/tissue compartment. The amount of midazolam available for intestinal metabolism was defined as the amount of midazolam in the acceptor and the cell/tissue compartment and the total amount of 1OH-midazolam as calculated above. In all systems, minor traces of 1OH-midazolam-glucoronide formation were detected, however in most experiments this was below or very close to the limit of quantification. We did therefore not consider the metabolite for further analysis.

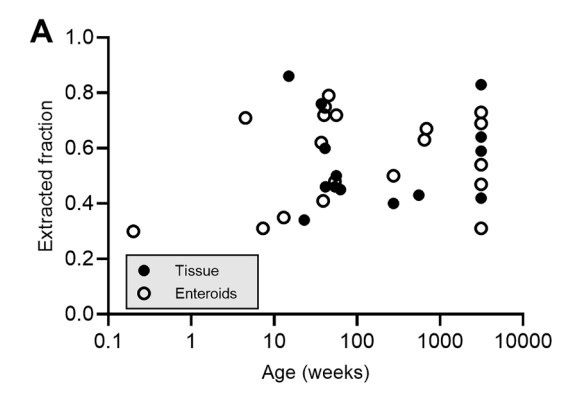
#### 2.10. Statistics

Data are presented in mean per donor for each experimental condition. Extracted fraction and gene expression correlations with age, in Fig. 2 and 3, were exploratively tested with Spearman correlation. In Fig. 4, apical and basolateral dosed metabolism was compared using a Wilcoxon signed rank test. Significance was reported when p < 0.05. Statistical analyses were performed using GraphPad Prism 8.0.1.

#### 3. Results

#### 3.1. CYP3A4/5 activity in tissue explants, enteroids and Caco-2 cells

In both adult enteroids and adult tissue explants (with Ussing chamber), total midazolam concentrations decreased gradually over time, while the main metabolite 10H-midazolam was produced simultaneously, indicative of CYP3A activity (Fig. 1A and B). A similar extraction fraction of midazolam was observed for enteroid monolayers  $(0.5\pm0.4,n=5)$  and intestinal tissues  $(0.6\pm0.4,n=4)$ , whereas the extraction fraction of Caco-2 was 40-fold lower  $(0.016\pm0.006,n=3)$  (Fig. 1C). This was in line with CYP3A4 gene expression levels, which was comparable between tissue explants and enteroids and low in Caco-2 cells (Fig. 1D). As further confirmation, midazolam metabolism was inhibited 2.8-fold by the prototypical CYP3A4 inhibitor ketoconazole in enteroid monolayers, indicating functionality of CYP3A4 in metabolite formation (Figure A.1). Results were also expressed as metabolic rate (pmol/mg protein/min), and can be found in Figure A.2.



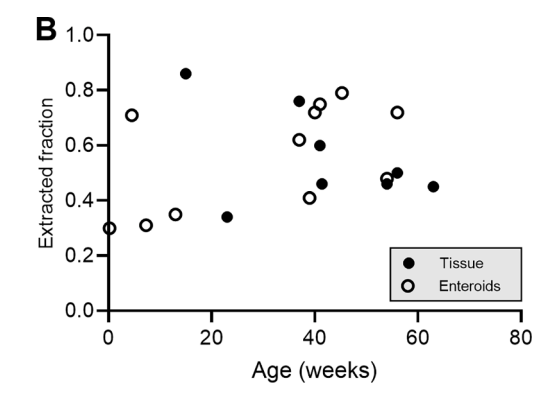


Fig. 2. Extracted fraction of midazolam *versus* age for tissue (closed dot) and enteroid monolayers (open dot). A: Extracted fraction in tissue and enteroids of all donors *versus* age (log scale). B: Extracted fraction in tissues and enteroids for donors <70 weeks old *versus* age (linear scale).

#### 3.2. Age-related CYP3A4/5 functionality and expression

Next, we investigated the suitability of enteroids to study age-related differences in midazolam metabolism and whether enteroids could serve as alternative model for fresh isolated tissue. Midazolam-extracted fractions were determined in enteroid monolayers of pediatric donors [median (range) age: 41 weeks (2 days - 13 years), n = 14] and in pediatric tissue (Ussing chamber) [median (range) age: 54 weeks (23 weeks - 10 years), n = 10]. The extraction fraction was within the same range with similar variation between donors in enteroid monolayers compared to tissue, both in pediatric and adult donors (Fig. 2A). No statistically significant relationship with age was observed for enteroids (r: -0.09, p = 0.420) or tissue (r: 0.20, p = 0.760) across the studied age range. As most maturational changes are expected to take place in the first year of life (van Groen et al., 2021b), we zoomed in on donors of 0 to 70 weeks old (Fig. 2B). Explorative statistics on the limited number of samples included in this age ranges showed a possible correlation with age in enteroid monolayers (r:0.67, p = 0.029). However, the number of donors was too low to draw solid conclusions. Paired extracted fraction in both enteroids and tissue was obtained for 5 out of 18 donors (Table A.1).

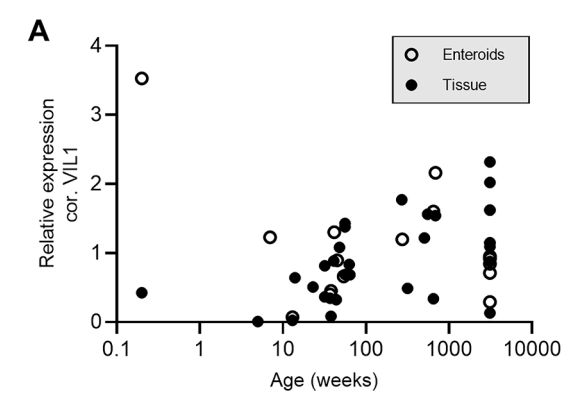
In total, it was possible to obtain 11 pediatric [median (range) age: 41 weeks (2 days – 13 year)] and 5 adult enteroid monolayers for RNA analysis. In tissue, expression of CYP3A4 was determined for 23 pediatric [median (range) age: 45 weeks (2 days - 13 year)], and 9 adult donors. Interestingly, CYP3A4 gene expression in intestinal tissue did increase with age (r: 0.58, p=0.0004). In the 0–70 weeks age group this trend was even more distinct (r: 0.63, p=0.008, Fig. 3A). In enteroids this could not be confirmed, likely due to the lower number of monolayers analyzed and the higher level of variation. Nevertheless, visually

a similar trend appeared to be present in the 0–70 weeks old age group, except for one outlier (Fig. 3B). For 9 out of 24 donors analyzed for gene expression, we obtained paired gene expression data in both enteroids and tissue. The number of paired donors was too small to draw any conclusions (Table A.1).

#### 3.3. Asymmetric intestinal metabolism

The appearance of metabolite 10H-midazolam was determined in the apical and basolateral compartments as well as within cells/tissues, for both children and adults. Interestingly, increased levels of midazolam metabolism were observed in both models when midazolam was dosed on the apical side, compared to dosing to the basolateral side (enteroids: pediatric p = 0.0001, adult p = 0.063, Fig. 4A; Tissue: pediatric p = 0.008, adult p = 0.063, Fig. 4B). In case of midazolam dosing on the apical side, larger amounts of 10H-midazolam appeared on the apical side (luminal side) of enteroid monolayers (66  $\pm$  7%) and the tissue explants (56  $\pm$  9%), compared to the other compartments (Fig. 4C+D). In contrast, when midazolam was dosed on the basolateral side in tissue, the appearance of total 10H-midazoalam was equal in the apical (19  $\pm$  6%) and basolateral compartment (24  $\pm$  7%), while most metabolite remained in the tissue segment (57  $\pm$  9%) during the two hours of the experiment (Fig. 4C). In enteroid monolayers, the distribution of 10H-midazolam in the basolaterally-dosed situation, is similar to the apically-dosed situation (Fig. 4D). Fig. 5 shows a schematic representation of observed asymmetric midazolam metabolism in tissues.

We hypothesized that this is the result of a more pronounced expression of CYP3A4 on the apical side of the cell. In addition, we hypothesized that due the presence of the lamina propria, asymmetrical distribution is more pronounced in tissue compared to cells. An apical



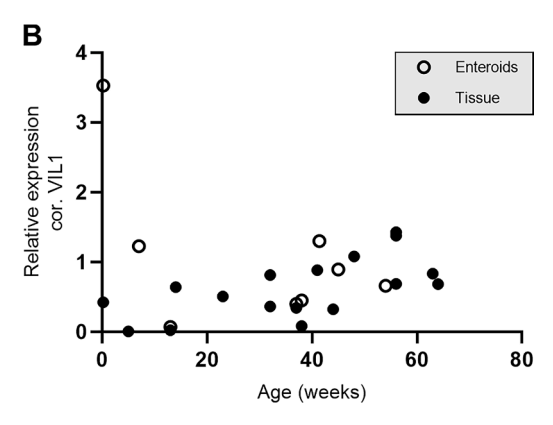


**Fig. 3.** Gene expression of CYP3A4 in tissue (closed dots) and enteroid monolayers (open dots) relative to Villin-1. A: Gene expression in tissues (n = 32) and enteroid monolayers (n = 16) of all donors on a log10 age scale. B: Relative expression in tissue and enteroid monolayers of donors <70 weeks on a linear age scale, tissue n = 17, enteroid monolayers n = 8.

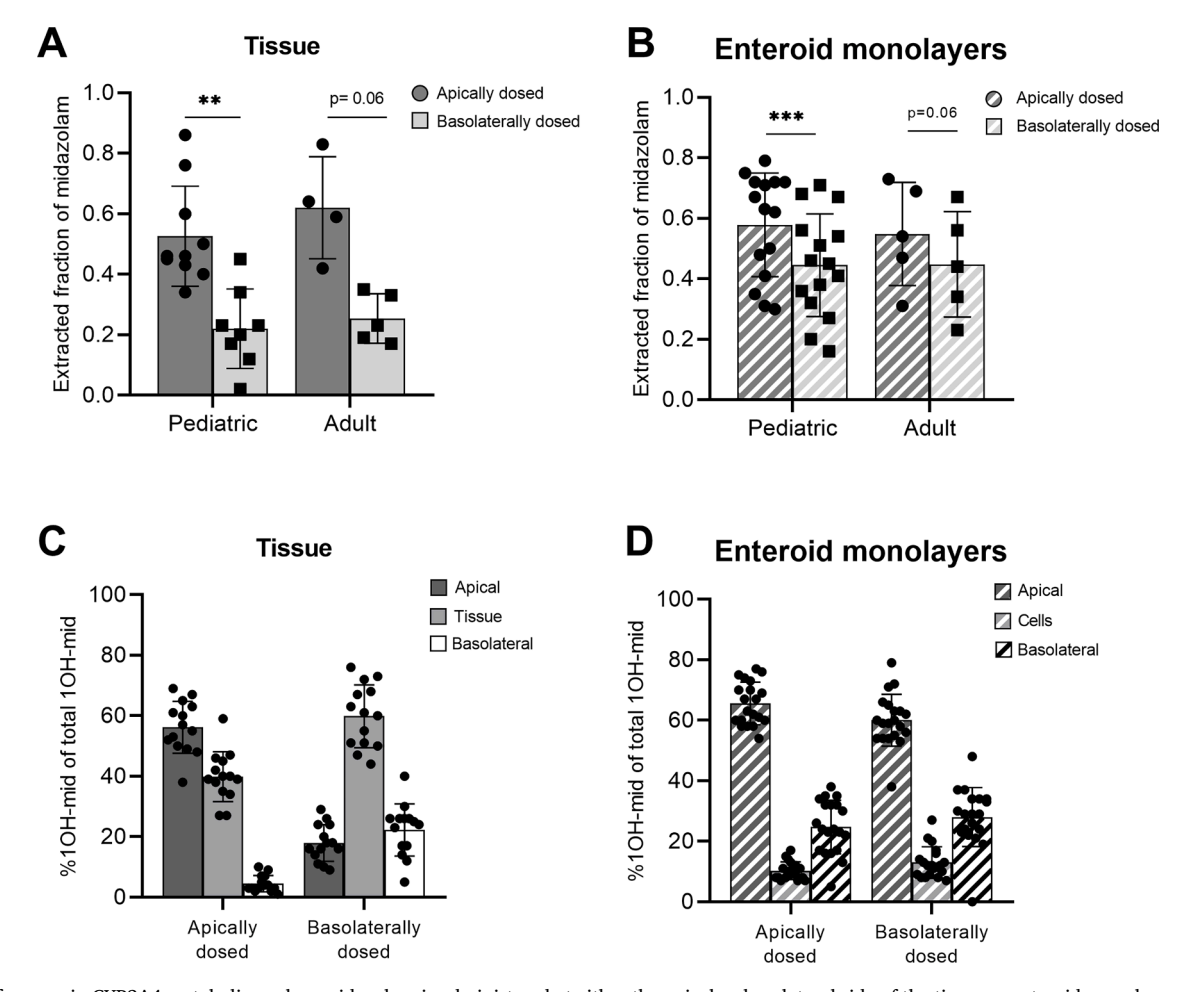


Fig. 4. Differences in CYP3A4 metabolism when midazolam is administered at either the apical or basolateral side of the tissue or enteroid monolayer. A: Extracted fraction in tissue in pediatric and adult donors in A-to-B and B-to-A dose direction. B: Extracted fraction in enteroid monolayers in pediatric and adult donors for the A-to-B and B-to-A dosing direction. C + D: Distribution of the 1OH-midazolam in% to total produced 1OH-midazolam of both pediatric and adult donors. In tissue (C) and in enteroid monolayers (D). \*\*: p < 0.01, \*\*\*: p < 0.0001.

localization of CYP3A4 in tissue was confirmed using immunofluorescent staining. Crypt cells in the intestinal tissue were negative for villin and CYP3A4. Not every cell of the enteroid monolayers showed CYP3A4 expression (Fig. 6). This corresponds to the cell heterogeneity observed in organoid cell lines.

#### 4. Discussion

We successfully cultured enteroid monolayers to study midazolam metabolism by CYP3A4/5 in pediatric and adult donors. The extracted fraction of midazolam using enteroid monolayers was similar to extraction fractions in the Ussing chamber experiments. Gene expression data showed age-related variation in CYP3A4 expression in tissue of pediatric donors. Next to that, metabolism by CYP3A4/5 was higher when midazolam was administered at the luminal side of the intestinal barrier in tissue and enteroids.

To the best of our knowledge, we are the first to directly compare drug metabolism between tissue derived enteroids and intestinal tissue. Enteroid monolayers and Ussing chamber experiments with adult tissue showed similar extraction fractions of midazolam after apical dosing, indicating that the enteroid monolayers maintained their metabolic capacity upon *in vitro* culturing, in contrast to Caco-2. Interindividual variation was within a similar range between the enteroid model and Ussing chamber. Our data shows a large interindividual variation in CYP3A activity and expression in the intestinal wall, thereby highlighting the importance to include this variation in drug metabolism

research.

This study presents opportunities to study ontogeny patterns in drug metabolizing enzyme activity with enteroids derived from children to elucidate existing knowledge gaps. Enteroids can be cultured from small volume biopsies, resulting in a less invasive and challenging opportunity to perform research with pediatric material. We explored the relationship between metabolic capacity with age in both enteroids and tissue. In enteroids, extracted fraction in the 0–70 weeks old age groups showed increased metabolism with age, however, not across the whole age range. Additionally, most enteroid CYP3A4 gene expression data points were within tissue expression variation, indicating that organoids might retain their age-related CYP3A4 capacity. In tissue, CYP3A4 gene expression was related to age, however, on a functional level (extracted fraction) this could not be confirmed. This was likely not possible because of the small size of the tissue available in the youngest age groups leading to a low number of successful Ussing chamber experiments. More donor inclusions, especially in the age group of 0-2 years old, are required for a robust study outcome to confirm these findings.

For intestinal CYP3A4 expression two ontogeny pattern theories exist (Johnson et al., 2023). Upreti and Wahlstrom in 2016 presented *in vitro* data suggesting a gradual increase with age, whereas whole body *in vivo* data showed a steep increase of CYP3A functionality until one year old, after which it slowly decreased to adult levels (Upreti and Wahlstrom, 2016). This might indicate that the *in vitro* models used (S9 fraction, microsomes) do not recapitulate the *in vivo* situation (Upreti and Wahlstrom, 2016). Tissue derived enteroids could overcome these

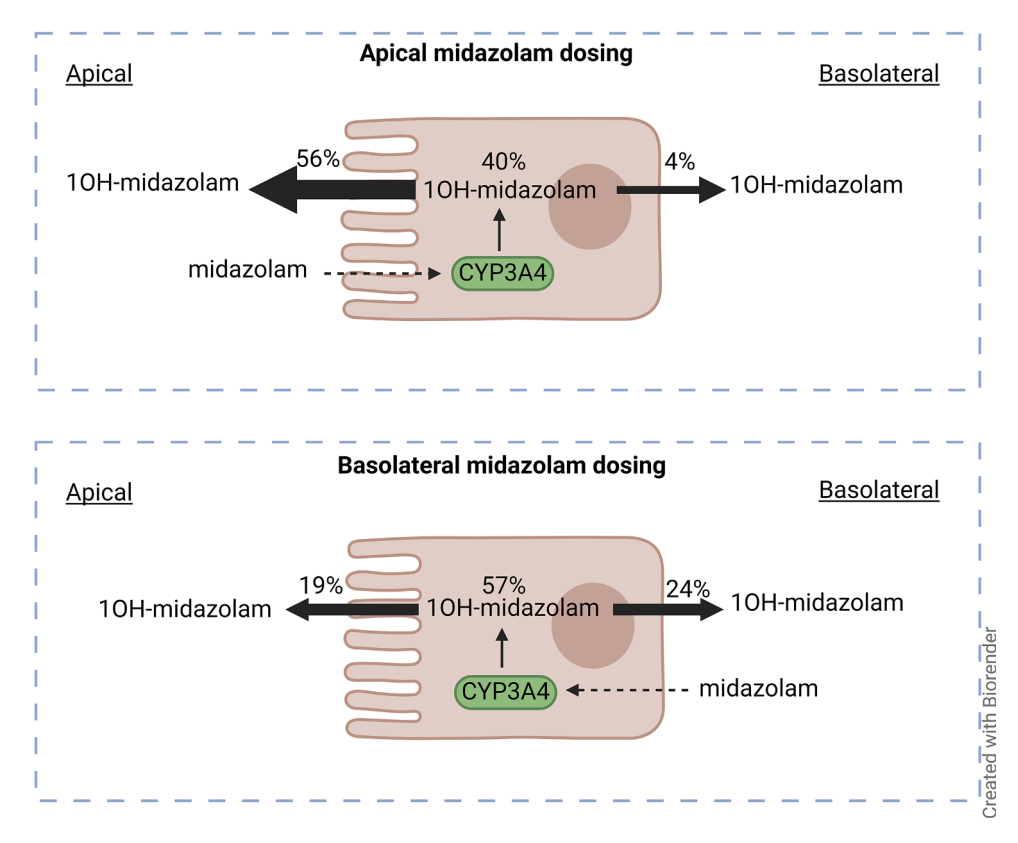


Fig. 5. Schematic representation of 10H-midazolam distribution after apical or basolateral dosing of midazolam to the tissue.

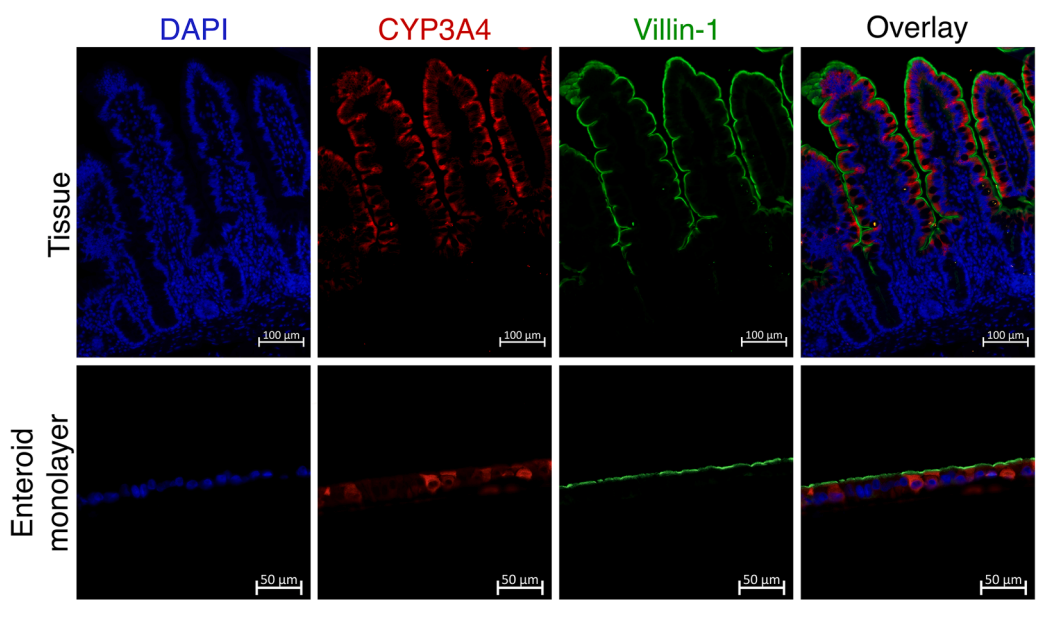


Fig. 6. CYP3A4 protein localization in adult intestinal tissue and adult enteroid monolayers, from left to right: DAPI (nuclei), CYP3A4, Villin-1, overlay of the three fluorescent channels.

limitations, if they represent the age-specific PK functionality of the donors. The other theory by Salem et al., 2014, proposes a linear increase in functionality after birth until adult levels after 1 year of age, which was obtained by deconvolution of clinical data (Salem et al., 2014). Both theories have been incorporated in PBPK models by Johnson et al., in 2023 (Johnson et al., 2023). They compared PBPK simulation output with an *in vivo* data set, showing that PBPK predictions based on Upreti's ontogeny profile performed better. In this study, CYP3A4 functionality increased with age in 0–70 week old donor

enteroid monolayers, and in tissue, expression of CYP3A4 linearly increased with age. However, too few samples were included to draw definitive conclusions. A linear trend with age was previously found in proteomics studies in duodenum and jejunum (Goelen et al., 2023; Kiss et al., 2021). Nevertheless, it should be considered that expression data does not directly predict protein functionality, therefore we also determined CYP3A4/5 functionality (Czuba et al., 2018; Drozdzik et al., 2018). This emphasizes the importance to understand every single piece of the puzzle to capture the total picture for pediatric PBPK modelling.

Interestingly, less metabolites were formed when midazolam was dosed to the basolateral side of the intestinal barrier compared to apically dosed midazolam. When added to the apical side, an asymmetric distribution between compartments of metabolite 10H-midazolam was observed in tissue. This behavior has been observed before for midazolam, *in vitro* as well as systemically in monkeys (Cummins et al., 2001; Nishimura et al., 2007; Paine et al., 1997). Staining of CYP3A4 in tissue showed the apical localization of CYP3A4 in the enterocytes. Together with the presence of the lamina propria this explains the more pronounced asymmetrical distribution in tissue compared to enteroid monolayers.

By using the fraction of midazolam absorbed that is metabolized, we could compare the two different intestinal models (enteroid monolayers and Ussing chamber). This extraction fraction was not influenced by area or mg protein present in the metabolizing model, which differ a lot between the two models (Nishimura et al., 2007; Paine et al., 1996). Typically, drug metabolism by enzymes is expressed as metabolic rate (pmol/mg protein/min), however, correcting for mg protein can lead to overcorrection in tissue when comparing to enteroid data (data in Figure A.1A) (Lipscomb and Poet, 2008). As a next step, we calculated 10H-midazolam production in pmol/cm2, to correct for surface area difference between the models (Figure A.1B). However, the metabolic rate is influenced by the number of cells present in the area of exposure. As the number of cells of 1 cm<sup>2</sup> exposed tissue is higher due to the presence of macro villi compared to enteroid monolayers, metabolic rate is higher in tissue (Figure A.1B). Taking into account that the enlargement factor of macro villi in the intestine is 4.3-4.5-fold in the ileum region, the metabolic rate of enteroid monolayers is more in line with tissue, however, still influenced by the number of cells (Figure A.1C) (Helander and Fandriks, 2014; Willmann et al., 2004; Wilson, 1967). Therefore, the extracted fraction makes it possible to study drug metabolism by CYP3A4 and directly compare fresh tissue with enteroid monolayers.

Both enteroid monolayer culturing and intestinal Ussing chamber experiments have their limitations. Fresh tissue pieces need to be large enough to be used in the Ussing chamber setup. Especially for the neonates this limited the number of usable tissue samples. Enteroids provide a possible solution for this problem, as they can be isolated and grown from smaller tissue pieces. Due to the challenging nature of both techniques only few paired experiments (Ussing chamber and monolayer from the same donor) were successful. Robust paired donor data from both models could help to compare study outcomes and establish whether tissue-specific CYP3A4/5 activity is retained in the resulting enteroids. All donor material used in this study was derived from hospitalized patients. Most donors >2 months old underwent surgery in a stable situation for lifting of their stoma, which was placed earlier during acute illness. In contrast, donor material from neonates <2 months of age was collected during mostly acute surgery. The underlying intestinal disease, including necrotizing enterocolitis, may have impacted the observed CYP3A4 expression and/or functionality and thereby affected the impact of age. Adult tissues were collected from hemicolectomy surgeries for colon cancer. Tissue surrounding cancer areas could have altered gene expression (Aran et al., 2017). As in previous studies, high variation between donors was observed (van Groen et al., 2021a).

In summary, we succeeded in culturing enteroid monolayers from both adult and pediatric donors. We showed that enteroids can be successfully used to study CYP3A4/5 metabolism. Extracted fractions of midazolam were comparable between tissue and enteroid monolayers. Our data suggest retainment of age-related functional expression of CYP3A4/5, which needs to be further explored in a larger study cohort. This study indicates that enteroids are a promising tool to study drug metabolism *in vitro* and potentially predict oral absorption for special populations as an alternative way to fresh tissue studies.

#### **Funding**

This work was supported by the Radboudumc, Junior researcher round 2020, Nijmegen, The Netherland

#### CRediT authorship contribution statement

Eva J. Streekstra: Writing – original draft, Visualization, Validation, Project administration, Methodology, Investigation, Formal analysis, Data curation. Marit Keuper-Navis: Writing – review & editing, Visualization, Validation, Methodology, Investigation. Jeroen J.W.M. van den Heuvel: Supervision, Methodology, Conceptualization. Petra van den Broek: Writing – review & editing, Methodology. Rick Greupink: Writing – review & editing, Validation, Supervision. Martijn W.J. Stommel: Methodology, Investigation. Willem P. de Boode: Methodology. Sanne M.B.I. Botden: Methodology, Conceptualization. Frans G.M. Russel: Writing – review & editing, Supervision, Investigation, Conceptualization. Evita van de Steeg: Writing – review & editing, Supervision, Project administration, Funding acquisition, Conceptualization. Saskia N. de Wildt: Writing – review & editing, Validation, Supervision, Project administration, Investigation, Funding acquisition, Data curation, Conceptualization.

#### Declaration of competing interest

All authors declared no competing interests for this work.

#### Data availability

Data will be made available on request.

#### Supplementary materials

Supplementary material associated with this article can be found, in the online version, at doi:10.1016/j.ejps.2024.106868.

#### References

- Altay, G., et al., 2019. Self-organized intestinal epithelial monolayers in crypt and villuslike domains show effective barrier function. Sci. Rep. 9, 10140. https://doi.org/
- Aran, D., et al., 2017. Comprehensive analysis of normal adjacent to tumor transcriptomes. Nat. Commun. 8, 1077. https://doi.org/10.1038/s41467-017-01027-7
- Braverman, J., Yilmaz, O.H., 2018. From 3D Organoids back to 2D Enteroids. Dev. Cell 44, 533–534. https://doi.org/10.1016/j.devcel.2018.02.016.
- Brussee, J.M., et al., 2018a. Predicting CYP3A-mediated midazolam metabolism in critically ill neonates, infants, children and adults with inflammation and organ failure. Br. J. Clin. Pharmacol. 84, 358–368. https://doi.org/10.1111/bcp.13459
- Brussee, J.M., et al., 2018b. First-pass CYP3A-mediated metabolism of midazolam in the gut wall and liver in preterm neonates. CPT Pharmacomet. Syst. Pharmacol. 7, 374–383. https://doi.org/10.1002/psp4.12295.
- Cummins, C.L., et al., 2001. Characterizing the expression of CYP3A4 and efflux transporters (P-gp, MRP1, and MRP2) in CYP3A4-transfected Caco-2 cells after induction with sodium butyrate and the Phorbol Ester 12-O-Tetradecanoylphorbol-13-Acetate. Pharm. Res. 18, 1102–1109. https://doi.org/10.1023/A: 1010914624111
- Czuba, L.C., et al., 2018. Post-translational modifications of transporters. Pharmacol. Ther. 192, 88–99. https://doi.org/10.1016/j.pharmthera.2018.06.013.
- de Waal, T., et al., 2024. Expression of intestinal drug transporter proteins and metabolic enzymes in neonatal and pediatric patients. Int. J. Pharm. 654, 123962 https://doi. org/10.1016/j.jipharm.2024.123962.
- de Wildt, S.N., et al., 2002. Pharmacokinetics and metabolism of oral midazolam in preterm infants. Br. J. Clin. Pharmacol. 53, 390–392. https://doi.org/10.1046/ i.1365-2125.2002.01223.x.
- Doherty, M.M., Charman, W.N., 2002. The mucosa of the small intestine. Clin. Pharmacokinet. 41, 235–253. https://doi.org/10.2165/00003088-200241040-00001.
- Driehuis, E., et al., 2020. Establishment of patient-derived cancer organoids for drug-screening applications. Nat. Protoc. 15, 3380–3409. https://doi.org/10.1038/s41596-020-0379-4.

- Drozdzik, M., et al., 2018. Protein abundance of clinically relevant drug-metabolizing enzymes in the human liver and intestine: a comparative analysis in paired tissue specimens. Clin. Pharmacol. Ther. 104, 515–524. https://doi.org/10.1002/cpt.967.
- Goelen, J., et al., 2023. Quantification of drug metabolising enzymes and transporter proteins in the paediatric duodenum via LC-MS/MS proteomics using a QconCAT technique. Eur. J. Pharm. Biopharm. 191, 68–77. https://doi.org/10.1016/j. eipb.2023.08.011.
- Gunasekara, D.B., et al., 2018. A monolayer of primary colonic epithelium generated on a scaffold with a gradient of stiffness for drug transport studies. Anal. Chem. 90, 13331–13340. https://doi.org/10.1021/acs.analchem.8b02845.
- Helander, H.F., Fandriks, L., 2014. Surface area of the digestive tract revisited. Scand. J. Gastroenterol. 49, 681–689. https://doi.org/10.3109/00365521.2014.898326.
- Johnson, T.N., et al., 2023. Use of developmental Midazolam and 1-hydroxymidazolam data with pediatric physiologically based modelling to assess CYP3A4 and UGT2B4 ontogeny in vivo. Drug Metab. Dispos. https://doi.org/10.1124/dmd.123.001270.
- Johnson, T.N., et al., 2001. Enterocytic CYP3A4 in a paediatric population: developmental changes and the effect of coeliac disease and cystic fibrosis. Br. J. Clin. Pharmacol. 51, 451–460. https://doi.org/10.1046/j.1365-2125.2001.01370.x.
- Kiss, M., et al., 2021. Ontogeny of small intestinal drug transporters and metabolizing enzymes based on targeted quantitative proteomics. Drug Metab. Dispos. 49, 1038–1046. https://doi.org/10.1124/dmd.121.000559.
- Kraiczy, J., et al., 2019. DNA methylation defines regional identity of human intestinal epithelial organoids and undergoes dynamic changes during development. Gut 68, 49–61. https://doi.org/10.1136/gutjnl-2017-314817.
- Lewis, S.K., et al., 2020. DNA methylation analysis validates organoids as a viable model for studying human intestinal. Aging Cell. Mol. Gastroenterol. Hepatol. 9, 527–541. https://doi.org/10.1016/j.jcmgh.2019.11.013.
- Lipscomb, J.C., Poet, T.S., 2008. In vitro measurements of metabolism for application in pharmacokinetic modeling. Pharmacol. Ther. 118, 82–103. https://doi.org/ 10.1016/j.pharmthera.2008.01.006.
- Mooij, M.G., et al., 2016. Human intestinal PEPT1 transporter expression and localization in preterm and term infants. Drug Metab. Dispos. 44, 1014–1019. https://doi.org/10.1124/dmd.115.068809.
- Mooij, M.G., et al., 2014. Ontogeny of human hepatic and intestinal transporter gene expression during childhood: age matters. Drug Metab. Dispos. 42, 1268–1274. https://doi.org/10.1124/dmd.114.056929.
- Nicolas, J.M., et al., 2017. Oral drug absorption in pediatrics: the intestinal wall, its developmental changes and current tools for predictions. Biopharm. Drug Dispos. 38, 209–230. https://doi.org/10.1002/bdd.2052.
- Nishimura, T., et al., 2007. Asymmetric intestinal first-pass metabolism causes minimal oral bioavailability of midazolam in cynomolgus monkey. Drug Metab. Dispos. 35, 1275–1284. https://doi.org/10.1124/dmd.106.013037.
- Paine, M.F., et al., 1997. Characterization of interintestinal and intraintestinal variations in human CYP3A-dependent metabolism. J. Pharmacol. Exp. Ther. 283, 1552–1562.
- Paine, M.F., et al., 1996. First-pass metabolism of midazolam by the human intestine. Clin. Pharmacol. Ther. 60, 14–24. https://doi.org/10.1016/S0009-9236(96)90162-01.
- Roodsant, T., et al., 2020. A human 2D primary organoid-derived epithelial monolayer model to study host-pathogen interaction in the small intestine. Front. Cell. Infect. Microbiol. 10, 272. https://doi.org/10.3389/fcimb.2020.00272.

- Salem, F., et al., 2014. A Re-evaluation and validation of ontogeny functions for cytochrome P450 1A2 and 3A4 Based on in vivo data. Clin. Pharmacokinet. 53, 625–636. https://doi.org/10.1007/s40262-014-0140-7.
- Sato, T., Clevers, H., 2013. Growing self-organizing mini-guts from a single intestinal stem cell: mechanism and applications. Science 340, 1190–1194. https://doi.org/ 10.1126/science.1234852 (1979).
- Sato, T., et al., 2011. Long-term expansion of epithelial organoids from human colon, adenoma, adenocarcinoma, and Barrett's epithelium. Gastroenterology 141, 1762–1772. https://doi.org/10.1053/j.gastro.2011.07.050.
- Scott, A., et al., 2016. Long-term renewable human intestinal epithelial stem cells as monolayers: a potential for clinical use. J. Pediatr. Surg. 51, 995–1000. https://doi. org/10.1016/j.jpedsurg.2016.02.074.
- Speer, J.E., et al., 2019a. Molecular transport through primary human small intestinal monolayers by culture on a collagen scaffold with a gradient of chemical crosslinking. J. Biol. Eng. 13, 36. https://doi.org/10.1186/s13036-019-0165-4.
- Speer, J.E., et al., 2019b. Evaluation of human primary intestinal monolayers for drug metabolizing capabilities. J. Biol. Eng. 13, 82. https://doi.org/10.1186/s13036-019-0212-1.
- Streekstra, E.J., et al., 2022. A proof of concept using the Ussing chamber methodology to study pediatric intestinal drug transport and age-dependent differences in absorption. Clin. Transl. Sci. 15, 2392–2402. https://doi.org/10.1111/cts.13368.
- Takenaka, T., et al., 2016. Application of a human intestinal epithelial cell monolayer to the prediction of oral drug absorption in humans as a superior alternative to the Caco-2 cell monolayer. J. Pharm. Sci. 105, 915–924. https://doi.org/10.1016/j. xpbs 2015.11.035
- Upreti, V.V., Wahlstrom, J.L., 2016. Meta-analysis of hepatic cytochrome P450 ontogeny to underwrite the prediction of pediatric pharmacokinetics using physiologically based pharmacokinetic modeling. J. Clin. Pharmacol. 56, 266–283. https://doi.org/ 10.1002/jcph.585.
- van den Anker, J., et al., 2018. Developmental changes in pharmacokinetics and pharmacodynamics. J. Clin. Pharmacol. 58 (Suppl 10), S10–S25. https://doi.org/ 10.1002/jcph.1284.
- van Groen, B.D., et al., 2021a. The oral bioavailability and metabolism of midazolam in stable critically Ill children: a pharmacokinetic microtracing study. Clin. Pharmacol. Ther. 109, 140–149. https://doi.org/10.1002/cpt.1890.
- van Groen, B.D., et al., 2021b. Ontogeny of hepatic transporters and drug-metabolizing enzymes in humans and in nonclinical species. Pharmacol. Rev. 73, 597–678. https://doi.org/10.1124/pharmrev.120.000071.
- Wang, Y., et al., 2017. Self-renewing monolayer of primary colonic or rectal epithelial cells. Cell. Mol. Gastroenterol. Hepatol. 4 https://doi.org/10.1016/j. icmgh.2017.02.011. 165-182 e167.
- Willmann, S., et al., 2004. A physiological model for the estimation of the fraction dose absorbed in humans. J. Med. Chem. 47, 4022–4031. https://doi.org/10.1021/ im030999b
- Wilson, J.P., 1967. Surface area of the small intestine in man. Gut 8, 618–621. https://doi.org/10.1136/gut.8.6.618.
- Yamashita, T., et al., 2021. Monolayer platform using human biopsy-derived duodenal organoids for pharmaceutical research. Mol. Therapy Methods Clin. Dev. 22, 263–278. https://doi.org/10.1016/j.omtm.2021.05.005.